On a new theoretical framework for RR Lyrae stars II: Mid–Infrared Period–Luminosity and Period–Wesenheit relations

Tizio, Caio

drafted May 29, 2015 / Received / Accepted

Received ______________________; accepted ______________________

ABSTRACT

abstract text

Subject headings: key1, key2

1. Introduction

2. Theoretical framework

To derive the MIR PL relations, we use the same models used by Marconi et al. (2015) to calculate the coefficients of optical and NIR PL relations. Since the models make predictions for seven different metallicities (Z = 0.0001, 0.0003, 0.0006, 0.001, 0.004, 0.008 and 0.0198) it is possible to derive the metallicity dependence of the zero-point.

REFERENCES

Marconi, M. , et al. 2015, ApJ, accepted

This manuscript was prepared with the AAS LaTeX macros v5.2.

Table 1. Theoretical NIR and MIR Period–Luminosity relations for RR Lyrae.

PLZ[a]	a[b] mag	b[b] mag	c[b] mag	σ[b] mag	a[c] mag	b[c] mag	c[c] mag	σ[c] mag	a[d] mag	b[d] mag	c[d] mag	σ[d] mag
		FO				FU				FU+FO		
					— Spitzer —							
IRAC1	-1.344	-2.718	0.152	0.021	-0.786	-2.276	0.184	0.035	-0.793	-2.251	0.180	0.037
	±0.024	±0.046	±0.004		±0.007	±0.021	±0.004		±0.007	±0.018	±0.003	
IRAC2	-1.348	-2.720	0.153	0.021	-0.775	-2.262	0.190	0.036	-0.785	-2.239	0.185	0.038
	±0.024	±0.046	±0.004		±0.007	±0.022	±0.004		±0.007	±0.018	±0.003	
IRAC3	-1.352	-2.724	0.153	0.021	-0.786	-2.273	0.188	0.035	-0.795	-2.250	0.184	0.037
	±0.023	±0.046	±0.004		±0.007	±0.021	±0.004		±0.007	±0.018	±0.003	
IRAC4	-1.355	-2.728	0.155	0.021	-0.798	-2.288	0.186	0.035	-0.805	-2.264	0.183	0.036
	±0.023	±0.046	±0.004		±0.007	±0.021	±0.004		±0.007	±0.017	±0.003	
					— WISE —							
WISE1	-1.341	-2.716	0.152	0.021	-0.784	-2.274	0.183	0.036	-0.790	-2.247	0.180	0.037
	±0.024	±0.047	±0.004		±0.007	±0.022	±0.004		±0.007	±0.018	±0.003	
WISE2	-1.348	-2.720	0.153	0.021	-0.774	-2.261	0.190	0.036	-0.784	-2.237	0.185	0.038
	±0.024	±0.046	±0.004		±0.008	±0.022	±0.004		±0.007	±0.018	±0.003	
WISE3	-1.357	-2.731	0.157	0.021	-0.800	-2.292	0.188	0.035	-0.807	-2.267	0.185	0.036
	±0.023	±0.045	±0.004		±0.007	±0.021	±0.004		±0.007	±0.018	±0.003	
WISE4	-1.355	-2.735	0.166	0.020	-0.799	-2.298	0.196	0.034	-0.805	-2.274	0.193	0.036
	±0.022	±0.044	±0.004		±0.007	±0.021	±0.004		±0.007	±0.017	±0.003	
					— HST/WFC3 —							
F110I	-0.892	-2.314	0.152	0.052	-0.365	-1.887	0.169	0.069	-0.357	-1.776	0.173	0.072
	±0.058	±0.114	±0.009		±0.014	±0.042	±0.007		±0.013	±0.035	±0.006	
F125I	-1.000	-2.396	0.153	0.048	-0.473	-1.976	0.170	0.060	-0.467	-1.880	0.174	0.064
	±0.053	±0.105	±0.009		±0.013	±0.036	±0.006		±0.012	±0.031	±0.006	
F160I	-1.216	-2.594	0.163	0.039	-0.686	-2.189	0.186	0.040	-0.688	-2.142	0.186	0.044
	±0.044	±0.086	±0.007		±0.008	±0.024	±0.004		±0.008	±0.021	±0.004	

[a]The PLZ relations of the form: M_X= a + b×log P + c×$[Fe/H]$.

[b]Zero–point (a), slope (b), metallicity term (c) and standard deviation (σ) for FO pulsators. The errors on the zero–point, slope and metallicity term are listed in the 2nd row.

[c]Zero–point (a), slope (b), metallicity term (c) and standard deviation (σ) for FU pulsators. The errors on the zero–point, slope and metallicity term are listed in the 2nd row.

[d]Zero–point (a), slope (b), metallicity term (c) and standard deviation (σ) for for the entire sample (FU+FO) of RR Lyrae. The periods of FO variables were fundamentalized by adopting the following relation: log P_F=log P_{FO}+0.127. The errors on the zero–point, slope and metallicity term are listed in the 2nd row.

Table 2. Theoretical MIR–Optical and MIR–NIR Period–Wesenheit relations for RR Lyrae.

PWZ[a]	x[b]	a[c]	b[c]	c[c]	σ[c]	a[d]	b[d]	c[d]	σ[d]	a[e]	b[e]	c[e]	σ[e]
		mag	mag	mag	mag	mag	mag	mag	mag	mag	mag	mag	mag
			FO				FU				FU+FO		
I1,B-I1	0.05	-1.436	-2.784	0.150	0.018	-0.883	-2.363	0.180	0.030	-0.891	-2.347	0.177	0.032
		±0.020	±0.040	±0.003		±0.006	±0.018	±0.003		±0.006	±0.015	±0.003	
I1,V-I1	0.07	-1.435	-2.786	0.152	0.018	-0.879	-2.358	0.184	0.030	-0.888	-2.345	0.180	0.032
		±0.020	±0.039	±0.003		±0.006	±0.018	±0.003		±0.006	±0.015	±0.003	
I1,R-I1	0.09	-1.430	-2.783	0.153	0.018	-0.873	-2.351	0.185	0.030	-0.882	-2.339	0.181	0.032
		±0.020	±0.040	±0.003		±0.006	±0.018	±0.003		±0.006	±0.015	±0.003	
I1,I-I1	0.13	-1.432	-2.785	0.153	0.018	-0.876	-2.354	0.186	0.030	-0.885	-2.343	0.181	0.032
		±0.020	±0.039	±0.003		±0.006	±0.018	±0.003		±0.006	±0.015	±0.003	
I2,B-I2	0.04	-1.417	-2.770	0.151	0.019	-0.848	-2.328	0.188	0.031	-0.858	-2.311	0.183	0.034
		±0.021	±0.041	±0.003		±0.007	±0.019	±0.003		±0.006	±0.016	±0.003	
I2,V-I2	0.05	-1.416	-2.771	0.153	0.019	-0.845	-2.323	0.191	0.032	-0.856	-2.309	0.185	0.034
		±0.021	±0.041	±0.003		±0.007	±0.019	±0.003		±0.006	±0.016	±0.003	
I2,R-I2	0.06	-1.412	-2.769	0.154	0.019	-0.840	-2.318	0.192	0.032	-0.851	-2.304	0.186	0.034
		±0.021	±0.041	±0.003		±0.007	±0.019	±0.003		±0.006	±0.016	±0.003	
I2,I-I2	0.09	-1.414	-2.770	0.154	0.019	-0.841	-2.319	0.192	0.032	-0.852	-2.306	0.187	0.034
		±0.021	±0.041	±0.003		±0.007	±0.019	±0.003		±0.006	±0.016	±0.003	
I1,J-I1	0.30	-1.426	-2.795	0.153	0.018	-0.869	-2.363	0.186	0.030	-0.879	-2.357	0.182	0.031
		±0.020	±0.039	±0.003		±0.006	±0.018	±0.003		±0.006	±0.015	±0.003	
I1,H-I1	0.58	-1.362	-2.732	0.150	0.022	-0.804	-2.297	0.182	0.034	-0.811	-2.270	0.179	0.036
		±0.024	±0.047	±0.004		±0.007	±0.021	±0.004		±0.007	±0.018	±0.003	
I1,K-I1	1.28	-1.309	-2.722	0.150	0.023	-0.745	-2.278	0.184	0.037	-0.752	-2.248	0.180	0.038
		±0.025	±0.050	±0.004		±0.008	±0.022	±0.004		±0.007	±0.019	±0.003	
I2,J-I2	0.21	-1.407	-2.776	0.154	0.019	-0.833	-2.322	0.194	0.032	-0.845	-2.312	0.187	0.034
		±0.021	±0.041	±0.003		±0.007	±0.019	±0.003		±0.006	±0.016	±0.003	
I2,H-I2	0.39	-1.361	-2.730	0.152	0.022	-0.783	-2.271	0.192	0.036	-0.793	-2.247	0.186	0.038
		±0.024	±0.047	±0.004		±0.007	±0.022	±0.004		±0.007	±0.018	±0.003	
I2,K-I2	0.76	-1.330	-2.723	0.152	0.022	-0.742	-2.253	0.195	0.038	-0.754	-2.227	0.189	0.040
		±0.025	±0.049	±0.004		±0.008	±0.023	±0.004		±0.007	±0.019	±0.004	
I2,I1-I2	3.32	-1.359	-2.726	0.155	0.021	-0.739	-2.217	0.212	0.042	-0.757	-2.197	0.202	0.044
		±0.024	±0.047	±0.004		±0.009	±0.025	±0.004		±0.008	±0.021	±0.004	

Table 2—Continued

PWZ[a]	x[b]	a[c]	b[c]	c[c]	σ[c]	a[d]	b[d]	c[d]	σ[d]	a[e]	b[e]	c[e]	σ[e]
		mag	mag	mag	mag	mag	mag	mag	mag	mag	mag	mag	mag

[a]The PWZ relations of the form: $W(M_1, M_2 - M_3)$= a + b×log P + c×$[Fe/H]$. $M_3 \neq M_1$ only for three-band Wesenheit magnitudes

[b]Color coefficient in Wesenheit magnitude: $x_{W(M_1,M_2-M_3)} = \frac{1}{A_{M_2}/A_{M_1} - A_{M_3}/A_{M_1}}$

[c]Zero–point (a), slope (b), metallicity term (c) and standard deviation (σ) for FO pulsators. The errors on the zero–point, slope and metallicity term are listed in the 2nd row.

[d]Zero–point (a), slope (b), metallicity term (c) and standard deviation (σ) for FU pulsators. The errors on the zero–point, slope and metallicity term are listed in the 2nd row.

[e]Zero–point (a), slope (b), metallicity term (c) and standard deviation (σ) for for the entire sample (FU+FO) of RR Lyrae. The periods of FO variables were fundamentalized by adopting the following relation: $\log P_F = \log P_{FO} + 0.127$. The errors on the zero–point, slope and metallicity term are listed in the 2nd row.

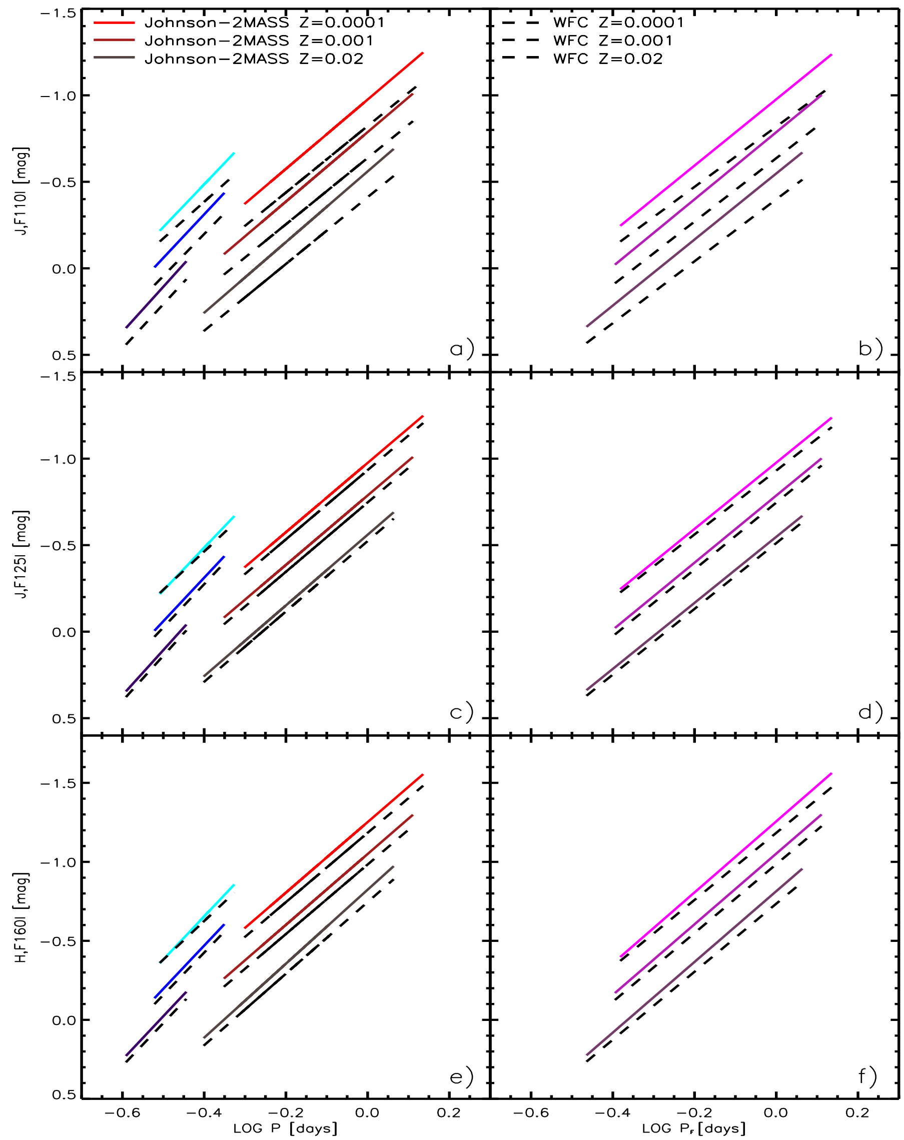

Fig. 1.— Comparison between WFC3 and 2MASS NIR PL relations. a): Lines of different colors display PL relations for FU and FO pulsators. The J and $F110IR$ PL relations are shown for a metallicity of Z=0.0001 (brighter), Z=0.001 (intermediate) and Z=0.0198 (fainter). b): Same as a), but for the entire sample of RR Lyrae models. The periods of FO models were fundamentalized using the relation: $\log P_{FU} = \log P_{FO} + 0.127$. Panels c) and d): Same as a) and b), but for the predicted J and $F125IR$ PL relations. Panels e) and f): Same as a) and b), but for the predicted H and $F160IR$ PL relations.

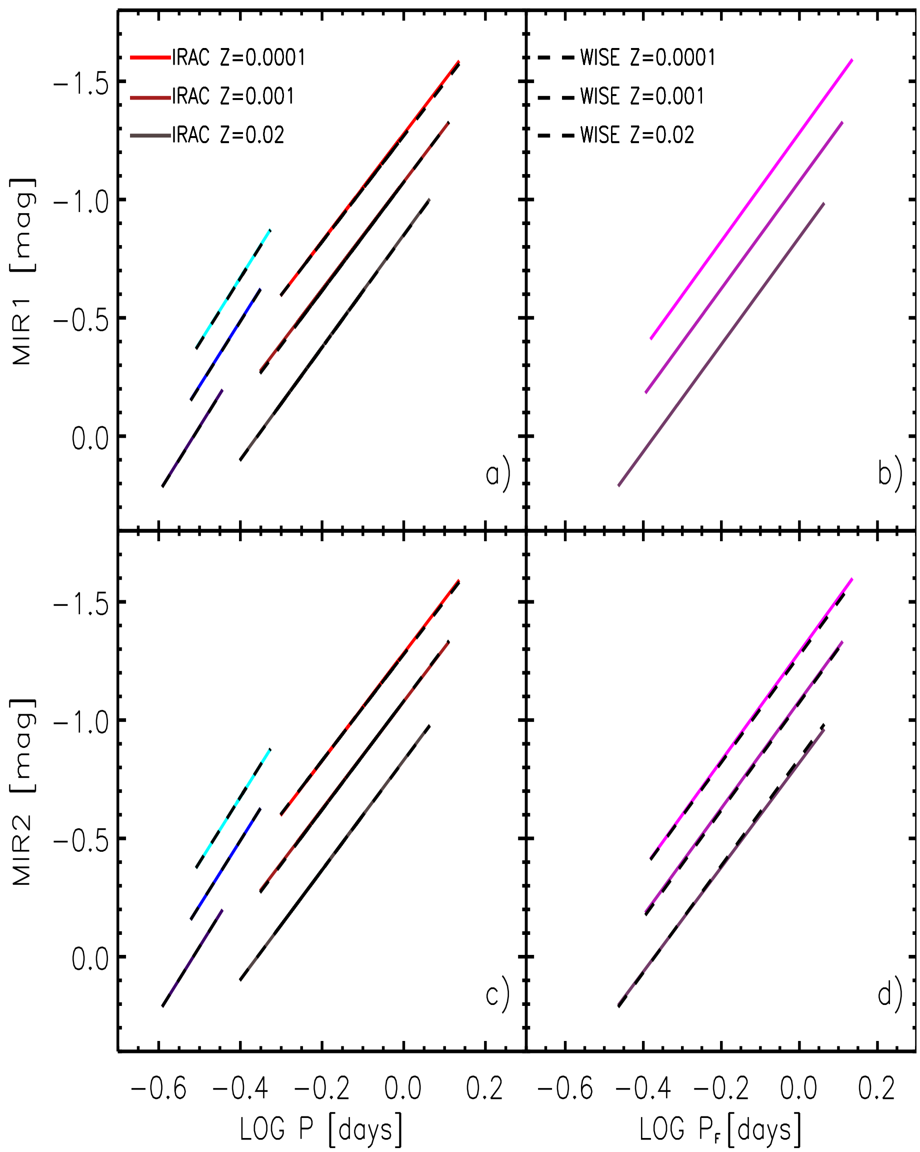

Fig. 2.— Comparison between IRAC and WISE MIR PL relations. a): Lines of different colors display PL relations for FU and FO pulsators. The $IRAC1$ and $WISE1$ PL are shown for a metallicity of Z=0.0001 (brighter), Z=0.001 (intermediate) and Z=0.0198 (fainter). b): Same as a), but for the entire sample of RR Lyrae models. The periods of FO models were fundamentalized using the relation: $\log P_{FU} = \log P_{FO} + 0.127$. Panels c) and d): Same as a) and b), but for the predicted $IRAC2$ and $WISE2$ PL relations.

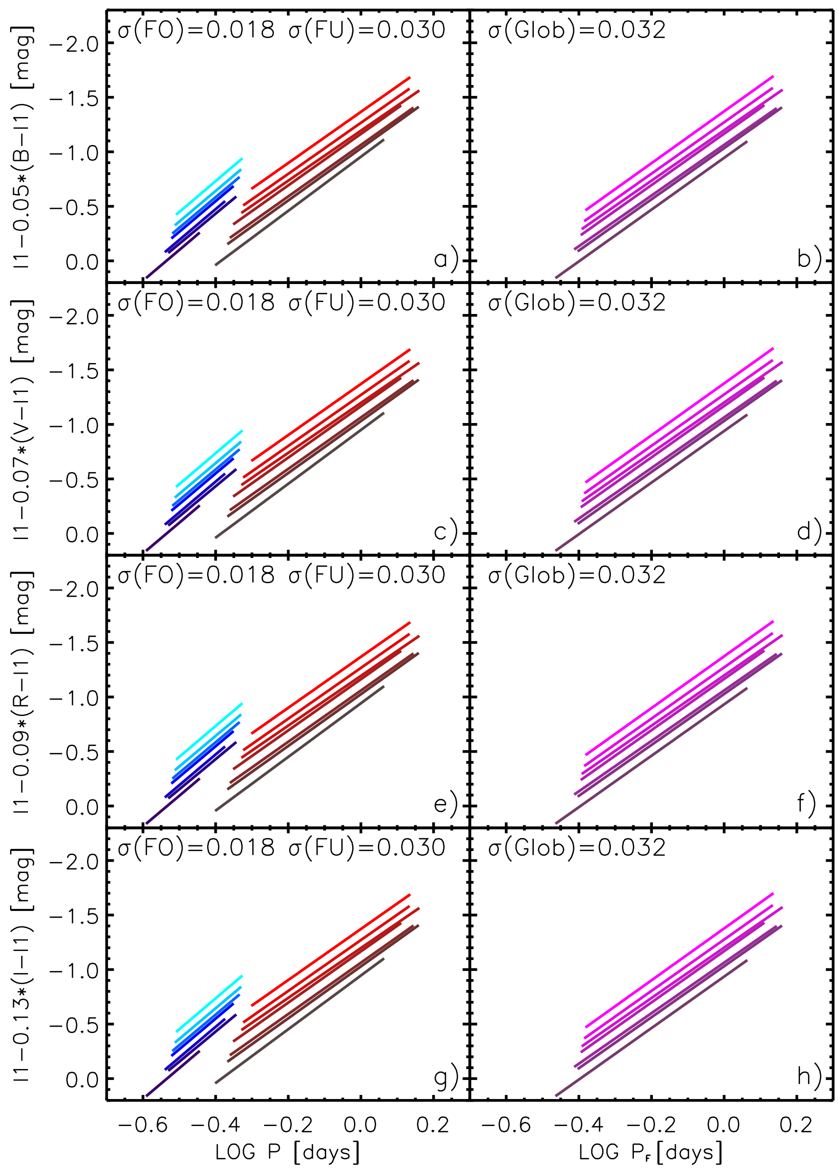

Fig. 3.— Optical–MIR PW relations. a): Lines of different colors display PW relations for FU and FO pulsators. The PW($I1,B-I1$) relations range in metallicity from Z=0.0001 (brighter) to Z=0.0198 (fainter). b): Same as a), but for the entire sample of RR Lyrae models. The periods of FO models were fundamentalized using the relation: $\log P_{FU}= \log P_{FO}+0.127$. Panels c) and d): Same as a) and b), but for the predicted $I1,V-I1$ PW relations. Panels e) and f): Same as a) and b), but for the predicted $I1,R-I1$ PW relations. Panels g) and h): Same as a) and b), but for the predicted $I1,I-I1$ PW relations.

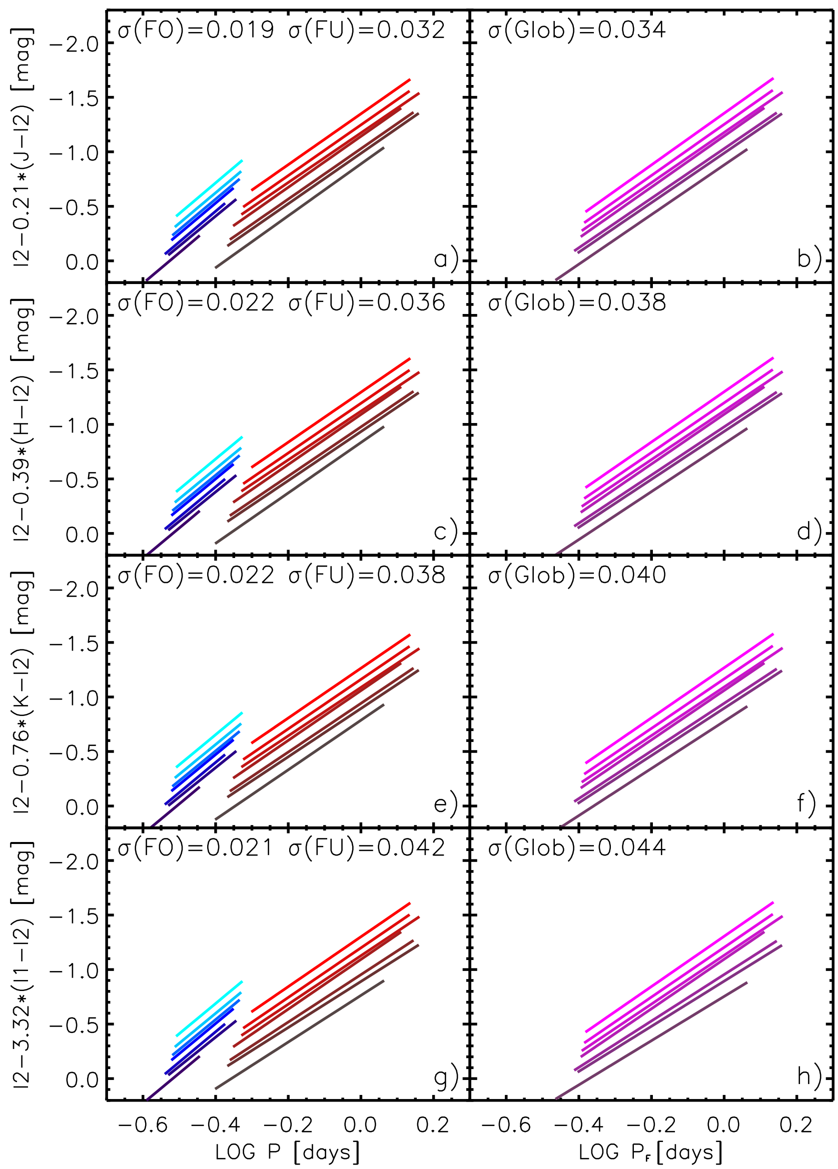

Fig. 4.— NIR–MIR PW relations. a): Lines of different colors display PW relations for FU and FO pulsators. The PW($I2$,$J-I2$) relations range in metallicity from Z=0.0001 (brighter) to Z=0.0198 (fainter). b): Same as a), but for the entire sample of RR Lyrae models. The periods of FO models were fundamentalized using the relation: $\log P_{FU}= \log P_{FO}+0.127$. Panels c) and d): Same as a) and b), but for the predicted $I2$,$H-I2$ PW relations. Panels e) and f): Same as a) and b), but for the predicted $I2$,$K-I2$ PW relations. Panels g) and h): Same as a) and b), but for the predicted $I2$,$I1-I2$ PW relations.

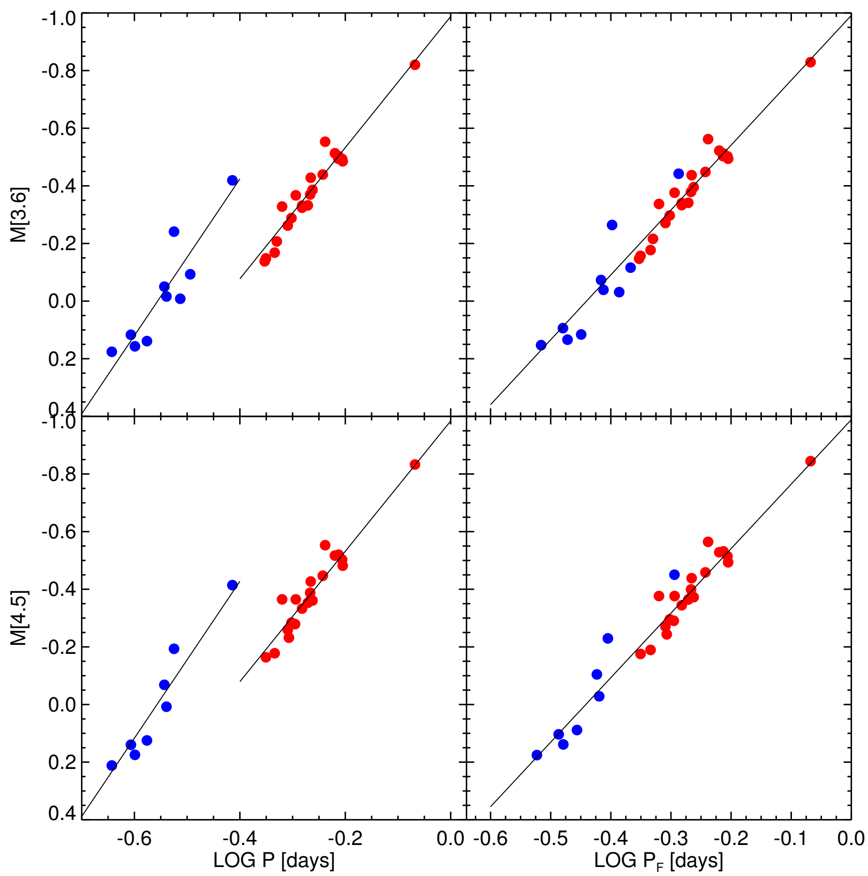

Fig. 5.— Observation of RR Lyrae stars in M4 fit to theoretical PLZ relation. Blue and red circles indicate FO and FU pulsators respectively.

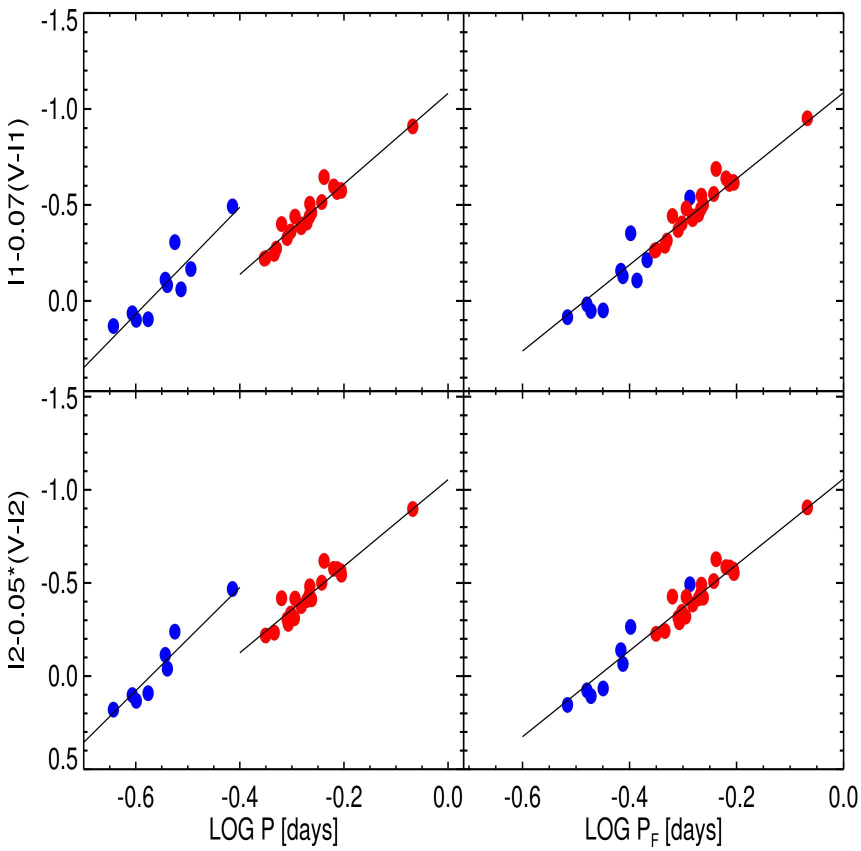

Fig. 6.— Observations of RR Lyrae stars in M4 fit to theoretical optical-MIR PW relations.